Title: STAP-2 interacts with and modulates BCR-ABL-mediated tumorigenesis

Authors: Yuichi Sekine, PhD[1,4], Osamu Ikeda, PhD[1,4], Akihiro Mizushima[1], Yusuke Ueno[1],Ryuta Muromoto, PhD[1], Akihiko Yoshimura, PhD[2], Yuzuru Kanakura, MD, PhD[3], Kenji Oritani, MD[3] and Tadashi Matsuda, PhD[1,5]

[1]Department of Immunology, Graduate School of Pharmaceutical Sciences Hokkaido University, Sapporo 060-0812, Japan, [2]Department of Microbiology and Immunology, Keio University School of Medicine, Shinjuku-Ku, Tokyo 160-8582, Japan, [3]Department of Hematology and Oncology, Graduate School of Medicine, Osaka University, 2-2 Yamada-oka, Suita, Osaka 565-0871, Japan

[4]These authors equally contributed to this work.

[5]Corresponding author: Dr. Tadashi Matsuda, Department of Immunology, Graduate School of Pharmaceutical Sciences, Hokkaido University, Kita-Ku Kita 12 Nishi 6, Sapporo 060-0812, Japan, TEL: 81-11-706-3243, FAX: 81-11-706-4990, E-mail: tmatsuda@pharm.hokudai.ac.jp

Running title: Functional interactions between STAP-2 and BCR-ABL

Word counts (excluding abstract, references and figure legends): 4,493

Abstract

In chronic myeloid leukemia (CML), the BCR-ABL fusion oncoprotein activates multiple pathways involved in cell survival, growth promotion and disease progression. In this report, we show that the signal transducing adaptor protein-2 (STAP-2) is involved in BCR-ABL activity. We demonstrate that STAP-2 bound to BCR-ABL, and BCR and ABL proteins, depending on the STAP-2 Src homology 2-like domain. BCR-ABL phosphorylates STAP-2 Tyr250 and the phosphorylated STAP-2 in turn up-regulated BCR-ABL phosphorylation, leading to enhanced activation of downstream signaling molecules including ERK, STAT5, BCL-xL and BCL-2. In addition, STAP-2 interacts with BCR-ABL to alter chemokine receptor expression leading to downregulation of CXCR4 and upregulation of CCR7. The interaction between STAP-2 and BCR-ABL plays a crucial role in conferring a growth advantage and resistance to imatinib, a BCR-ABL inhibitor, as well as tumor progression. Notably, mice injected with BCR-ABL/STAP-2-expressing Ba/F3 cells developed lymph node enlargement and hepatosplenomegaly. Moreover, suppression of STAP-2 in K562 CML cells resulted in no tumor formation in mice. Our results demonstrate a critical contribution of STAP-2 in BCR-ABL activity, and suggest that STAP-2 might be an important candidate for drug development for patients with CML. Further, the expression of STAP-2 provides useful information for estimating the characteristics of individual CML clones.

Keywords: chronic myeloid leukemia; BCR-ABL; signal transducing adaptor protein-2; chemokine; tumorigenesis

Introduction

The BCR-ABL fusion oncogene is responsible for the pathogenesis of chronic myelogenous leukemia (CML) (Quintas-Cardama and Cortes 2009), which is characterized by the premature release of myeloid cells from bone marrow as well as a substantial accumulation of myeloid cells in the blood, spleen and bone marrow. Owing to its elevated tyrosine kinase activity, BCR-ABL activates a number of signaling pathways, including the Ras, PI3K/Akt, Janus kinase/signal transducer and activator of transcription and NF-κB signaling pathways (Quintas-Cardama and Cortes 2009, Ren 2005). Moreover, in various human and mouse models, hematopoietic cells expressing BCR-ABL show a growth advantage, resistance to apoptosis, and altered adhesion and homing properties. In clinical research, tyrosine kinase inhibitors targeting BCR-ABL have dramatically improved the therapeutic outcomes of patients with CML (Corbin et al 2003, Gambacorti-Passerini et al 2003b, Gorre et al 2001, Hochhaus and La Rosee 2004, Lowenberg 2003, Shah et al 2002). For instance, the agent imatinib mesylate led to a large number of cytogenic and molecular responses in CML patients, resulting in greatly prolonged survival. However, a considerable proportion of these patients exhibited either primary or secondary resistance, or intolerance to imatinib (Cortes et al 2007). In addition, in a multicenter, non-randomized Stop Imatinib trial, approximately 60% of the patients relapsed after an interruption to the imatinib-therapy although they had maintained a complete molecular response (Mahon et al 2010). Thus, additional strategies to completely eliminate CML cells, especially leukemic stem cells, are necessary.

Signal transducing adaptor protein-2 (STAP-2) is a novel adaptor molecule, which was isolated as a c-fms-interacting protein (Minoguchi et al 2003). The human homologue of STAP-2 is a known substrate of the breast tumor kinase (Mitchell et al 2000). Structurally, STAP-2 contains a pleckstrin homology (PH) domain in the N-terminal region and a region distantly related to the Src homology 2 (SH2) in the central region. Its C-terminal region also has a proline-rich region and an

YXXQ motif (Minoguchi et al 2003). Previous works in this laboratory found that STAP-2 have the ability to associate with and influence a variety of signaling or transcriptional molecules, (Minoguchi et al 2003, Sekine et al 2005, Sekine et al 2006, Sekine et al 2007b, Sekine et al 2009a, Yamamoto et al 2003) including the finding that STAP-2 can modulate the transcriptional activity of STAT3 and STAT5 (Minoguchi et al 2003, Sekine et al 2005), in addition to the FcεRI and Toll-like receptor-mediated signals (Sekine et al 2006, Yamamoto et al 2003). Further, thymocytes and peripheral T cells from STAP-2-deficient mice show enhanced IL-2- or TCR-dependent cell growth, integrin-mediated T-cell adhesion and impaired SDF-1α-induced T-cell migration (Sekine et al 2005, Sekine et al 2007b, Sekine et al 2009a). Because STAP-2 is expressed in a variety of tissues and cells, such as lymphocytes, macrophages and hepatocytes, STAP-2 is also likely to function in a variety of different cells.

In this study, we identified BCR-ABL, in addition to BCR and ABL as novel binding partners of STAP-2. In the presence of STAP-2, BCR-ABL was highly phosphorylated. In parallel, the associated down-stream signals were also enhanced. We also found that STAP-2 overexpression in murine hematopoietic cells confers a growth advantage *in vitro* and is able to induce leukemia *in vivo*. In addition, STAP-2 controls the migration and homing of BCR-ABL-expressing cells by influencing chemokine receptor expression levels. Therefore, STAP-2 is required for the full activity of BCR-ABL.

Results

STAP-2 binds to BCR-ABL in addition to BCR and ABL proteins

To fully identify the STAP-2 interacting proteins, we used a yeast two-hybrid system to screen a mouse embryo cDNA library using human STAP-2 (amino acids 1-403) as the bait. From a total population of about 2.6×10^6 transformants, we isolated several positive clones. Sequence analysis revealed that one encoded the C-terminal region of BCR (amino acids 880-1270). We then examined whether STAP-2 binds to BCR in mammalian cells. A series of 293T cells were transfected with GST-tagged STAP-2 expression vectors together with Myc-tagged BCR (amino acids 880-1270). The specific binding was examined via pull-down assays with glutathione-sepharose, followed by western blot analysis with an anti-Myc or anti-GST antibody. The GST-STAP-2 protein precipitates clearly contained the BCR protein (Figure 1a), indicating that STAP-2 directly interacts with BCR in 293T cells. Because the BCR fragment in part overlapped with the BCR-ABLp210 chimera protein sequence (Pendergast et al 1991, Quintas-Cardama and Cortes 2009, Ren 2005), we also investigated whether STAP-2 interacts with the BCR-ABL oncoprotein. We then transfected the 293T cells with expression vectors encoding BCR-ABL (p210 or p190) and Myc-tagged STAP-2. The transfectants were then lysed and subjected to immunoprecipitation with an anti-Myc antibody. The immunoprecipitates were then run on a western blot with an anti-ABL antibody. As shown in Figure 1b, STAP-2 bound to both BCL-ABL p210 and p190. The binding between STAP-2 and BCR-ABLp190 was unexpected because BCR-ABLp190 is composed of BCR (amino acids 1-426). This finding raised the possibility that STAP-2 may recognize not only BCR but also ABL. Thus, we investigated whether STAP-2 interacts with the ABL protein. We transfected the 293T cells with the Myc-tagged STAP-2 and His-tagged ABL and the transfectants were then lysed and subjected to immunoprecipitation with an anti-ABL antibody. The precipitates for ABL contained the STAP-2 proteins (Figure 1c), indicating that STAP-2 directly interacts with ABL. To further detect a physical interaction between STAP-2 and BCR-ABL in the CML cells, co-immunoprecipitation

experiments were performed using a CML cell line K562, which constitutively expresses STAP-2. As shown in Figure 1d, we were able to demonstrate a direct interaction between STAP-2 and BCR-ABL at endogenous levels through the detection of BCR-ABL in the human CML cells (K562) after immunoprecipitation with a human STAP-2 antibody. Therefore, STAP-2 interacts with BCR-ABL as well as the BCR and ABL proteins. We further examined whether the interaction between STAP-2 and BCR-ABL depends on BCR-ABL phosphorylation. To this end, we first investigate the effect of BCR-ABL phosphorylation in the Ba/F3 transfectants by treatment with STI571. Treatment with STI571 resulted in a marked decrease of BCR-ABL phosphorylation in the Ba/F3 transfectants (p210 and p210/STAP-2#1) (Supplementary Figure 1a). We next tested the effect of treatment with STI571 on the interaction between STAP-2 and BCR-ABL. We then transfected the 293T cells with expression vectors encoding BCR-ABL (p210) and Myc-tagged STAP-2. The transfectants were treated or untreated with STI571, and then lysed and subjected to immunoprecipitation with an anti-Myc antibody. The immunoprecipitates were then run on a western blot with an anti-ABL antibody. Treatment with STI571 reduced the complex formation between STAP-2 and BCL-ABL p210 (Supplementary Figure 1b). Therefore, full recognition of BCR-ABL by STAP-2 requires BCR-ABL phosphorylation.

STAP-2 enhances BCR-ABL activity

To examine the effect of STAP-2 on the function of BCR-ABL, we stably transfected a STAP-2 expression vector into Ba/F3 cells expressing BCR-ABL (Ba/F3-p210). Western blot was used to confirm STAP-2 and BCR-ABL protein expression in the two clones (STAP-2WT#1 and #2)(see Figure 2c). Both STAP-2WT#1 and #2 showed markedly enhanced BCR-ABL-dependent cell growth and resistance to a BCR-ABL inhibitor, STI571 (Figures 2a, b). This finding suggests that STAP-2 positively regulates the BCR-ABL-dependent Ba/F3 cell growth. To investigate the molecular mechanisms underlying this process, we first examined tyrosine phosphorylation in the Ba/F3 transfectants. As shown in Figure 2c, intracellular tyrosine phosphorylation was markedly enhanced in the STAP-2WT#1 and #2 cells in the absence or presence of IL-3. The highly

enhanced bands were noted for BCR-ABL (Figure 2d) and STAT5 (Figure 2e).

Activation of downstream signaling molecules including ERK, STAT5, BCL-xL or BCL-2 was also enhanced in the STAP-2 WT#1 and #2 cells (Figure 2c). Furthermore, cell cycle analysis with flow cytometry showed that STAP-2 overexpression significantly suppressed the appearance cells at the sub-G1 phase 24 h after the depletion of IL-3 (Figure 2f), indicating that in these cells STAP-2 also augments the inhibition of apoptosis induced by BCR-ABL. Therefore, STAP-2 enhanced BCR-ABL phosphorylation results in a growth advantage and enhanced cell survival. To clarify the role of endogenous STAP-2 and BCR-ABL, we used a CML cell line K562, which constitutively expresses STAP-2. We first established a STAP-2-knockdown variant of the K562 cells using shRNA (K562 STAP-2 shRNA #1 and #2), in which the STAP-2 expression was confirmed with western blot (Figure 3a). Our findings revealed that cell proliferation in the K562 STAP-2 shRNA #1 and #2 cells was slower than in the control K562 cells (Figure 3b). In addition, the STAP-2-knockdown clones were more sensitive to STI571 than the controls (Figure 3c). When tyrosine phosphorylation was examined in the STAP-2 shRNA cells, a decrease in tyrosine phosphorylation in the cytoplasm was also observed (Figure 3d). We could see some alteration in Ptyr bands around M.W.100 kDa. Further, the phosphorylation status of the BCR-ABL downstream a signaling molecules, STAT5b was also diminished (Figure 3e). We then analyzed effects of STAP-2 knockdown on tyrosine-phosphorylation of STAT5 as well as CBL and VAV whose M.W. is around 100 kDa and their activation by BCR-ABL was already reported (Brehme et al 2009, Chang et al 2009). As shown in a new Figure 3f, tyrosine-phosphoryaltion of both CBL and VAV also reduced in STAP-2 knockdown K562 cells. We also tested the mRNA expression of STAT5b, BCL-2, BCL-xL and CYCLIN D1 in the STAP-2-knockdown K562 cells (shSTAP-2#1 and #2). As shown in Figure 3g, the mRNA expression of these proteins was significantly downregulated in STAP-2-knockdown cells as compared with the vector control cells (shControl #1 and #2). Therefore, at the physiological levels, interactions between STAP-2 and BCR-ABL play a crucial role in the control of BCR-ABL activity.

The SH2 domain of STAP-2 binds to BCR-ABL

To determine the STAP-2 domains involved in its association with BCR-ABL a series of STAP-2 deletion mutants fused with GST (GST-STAP-2 PH, GST-STAP-2 SH2 and GST-STAP-2 C) were examined (Figure 4a). The respective mutants, together with BCR-ABL, were transiently expressed in 293T cells. The binding potential of these proteins with BCR-ABL were examined by pull-down assays with glutathione-sepharose, followed by western blot analysis with anti-ABL or anti-GST antibodies. The precipitates for the GST-STAP-2 WT and GST-STAP-2 SH2 protein contained the BCR-ABL protein (Figure 4b). Therefore, STAP-2 interacts with BCR-ABL through a SH2-like domain.

Roles of the SH2 domain of STAP-2 in interactions between STAP-2 and BCR-ABL

We tested the effect of the SH2-like domain of STAP-2 on BCR-ABL-induced cell proliferation by using Ba/F3-p210 cells overexpressing STAP-2 ΔSH2, which lacks an SH2-like domain. As shown in Figures 4c and d, STAP-2 ΔSH2 #1 and #2 cells did not show any enhancement of BCR-ABL-dependent cell growth or resistance to STI571, although the STAP-2 WT and ΔSH2 expression levels were comparable (data not shown). In contrast to a STAP-2 WT clone, STAP-2 ΔSH2 #1 and #2 cells failed to have any significant effect on the phosphorylation of BCR-ABL (Figures 4e and 4f). We also examined whether STAP-2 SH2-like domain plays an important role in interactions between STAP-2 and BCR-ABL. As shown in Figure 4g, the immunoprecipitates with an anti-Myc antibody from cell lysates of Ba/F-p210/STAP-2 WT cells contained BCR-ABL protein. However, those from Ba/F-p210/STAP-2 ΔSH2 cells did not contain BCR-ABL protein. Thus, STAP-2 directly bound to BCL-ABL via its SH2-like domain. Therefore, the SH2 domain of STAP-2 is essential for physical and functional interactions between STAP-2 and BCR-ABL, leading to the enhanced BCR-ABL activity.

BCR-ABL phosphorylates STAP-2 at the position of Tyr250

STAP-2 has four tyrosine residues. To determine the phosphorylation status of these residues, we examined tyrosine phosphorylation of STAP-2 using BCR-ABL. The Myc-tagged STAP-2 was expressed without or with BCR-ABL in 293T cells. The cells were lysed, and the lysates were probed with anti-phosphotyrosine (PY), anti-Myc or anti-ABL antibodies. As shown in Figures 5a and 5b, a significant degree of tyrosine phosphorylation of STAP-2 by BCR-ABLp190 and p210 was observed. We also utilized a series of STAP-2 YF mutants in which four potential tyrosine phosphorylation sites were mutated to phenylalanine (Figure 5c). To further probe the phosphorylation status of STAP-2 Tyr250, we also used a phospho-specific antibody against the Tyr250 site, designated anti-pSTAP-2 Tyr250, as described previously.(Sekine et al 2007a) The Myc-tagged wild-type STAP-2 (STAP-2 WT) and a series of STAP-2 YF mutants were expressed with or without BCR-ABL in the 293T cells. The STAP-2 WT and YF mutant proteins expressed in the cells were then immunoblotted using anti-pSTAP-2 Tyr250, anti-PY and anti-Myc antibodies. The STAP-2 WT and YF mutant proteins, with or without BCR-ABL co-expression, were expressed at an equivalent level. In contrast, the anti-pSTAP-2 Tyr250 or anti-PY antibody failed to recognize the STAP-2 Y250F mutant co-expressed with BCR-ABL (Figures 5d, e). Therefore, STAP-2 Tyr250 is the major site of tyrosine phosphorylation by BCR-ABL.

The role of Tyr250 in interactions between STAP-2 and BCR-ABL

We also tested the effect of STAP-2 Tyr250 on BCR-ABL-induced cell proliferation by using Ba/F3-p210 cells overexpressing STAP-2 Y250F whose tyrosine residue at amino acid 250 was substituted to phenylalanine. In contrast to the STAP-2 WT clone, STAP-2 Y250F #1 and #2 cells did not show a significant enhancement of BCR-ABL-dependent cell growth and resistance to STI571 (Figures 5f, g), although the STAP-2 WT and Y250F expression levels were comparable (data not shown). Furthermore, tyrosine phosphorylation of a number of cellular proteins, including BCR-ABL itself, was only moderately enhanced in the STAP-2 Y250F #1 and #2 cells relative to the STAP-2 WT #2 cells (Figures 5h, i). Therefore, tyrosine phosphorylation of STAP-2 Tyr250 is

required for full enhancement of BCR-ABL activity.

BCR-ABL and BCR-ABL/STAP-2-expressing Ba/F3 cells show differing patterns of tumor progression

To investigate the effect of STAP-2 on the ability of transfected cells to induce tumor formation *in vivo*, we subcutaneously injected Ba/F3 transfectants into the flank of BALB/c nude mice. As shown in Figure 6a, the Ba/F3-p210 cells were lethal to the mice within 43.2 d. Importantly, lethality was augmented in the Ba/F3 cells expressing both BCR-ABL and STAP-2 (all mice died within 31 d). Mice injected with the vector control cells had no evidence of disease for at least 90 d. These results indicate that STAP-2 enhances BCR-ABL-mediated tumor progression *in vivo*. Mice injected with BCR-ABL-expressing Ba/F3 cells formed large tumors at the injection site (Figures 6b, c). However, these mice developed only small lymph node and spleen swelling (Figure 6d). Surprisingly, mice injected with BCR-ABL/STAP-2-expressing Ba/F3 cells developed small tumors at the injection sites but substantial lymph node swelling and hepatosplenomegaly (Figures 6b-d). The difference in tumor progression was also confirmed by the variable tumor weights observed between the groups (Figure 6e). In addition, the livers harvested from the mice injected with BCR-ABL/STAP-2-expressing, but not BCR-ABL-expressing Ba/F3 cells, showed a massive infiltration of tumor cells with hepatic necrosis (Figure 6f). Therefore, STAP-2 influences the migration and homing of BCR-ABL-expressing Ba/F3 cells.

Suppression of STAP-2 in K562 CML cells fails to form tumors in vivo

To further investigate the effect of STAP-2 in K562 CML on the ability to induce tumor formation *in vivo*, we subcutaneously injected K562 transfectants (K562 control shRNA #1 and K562 STAP-2 shRNA #1) into the flank of BALB/c nude mice. Mice injected with K562 control shRNA #1 cells formed large tumors at the injection site (Figures 7a, b, c), although we could not observe any metastasis in this model. Importantly, mice injected with K562 STAP-2 shRNA #1 cells failed to form tumors (Figures 7a, b, c). The difference in tumor formation was also confirmed by the

tumor weights observed between the groups (Figure 7d). Therefore, STAP-2 influences the migration and homing of BCR-ABL-expressing Ba/F3 cells.

STAP-2 cooperates with BCR-ABL to modify the expression of chemokine receptors

We previously showed that STAP-2 regulates SDF-1α-induced T-cell migration via activation of Vav1/Rac1 signaling, suggesting that STAP-2 may be involved in chemokine functions (Sekine et al 2009a). To clarify the tumor progression between BCR-ABL/STAP-2 and BCR-ABL-expressing Ba/F3 cells, we examined the mRNA expression levels of a series of chemokine receptors in the Ba/F3 transfectants. The mRNA expression of CCR1, CCR7 and CXCR1 was higher in the BCR-ABL/STAP-2-expressing Ba/F3 cells than in the BCR-ABL-expressing Ba/F3 cells (Figure 8a). In contrast, mRNA expression of CXCR4 was downregulated by STAP-2 (Figure 8a). We also tested the mRNA expression of these chemokine receptors in the STAP-2-knockdown K562 cells (shSTAP-2#1 and #2). As shown in Figure 8b, the mRNA expression of CCR1 and CCR7 was downregulated in STAP-2-knockdown cells as compared with the vector control cells (shControl #1 and #2), whereas mRNA expression levels of CXCR4 were strongly upregulated in the STAP-2-knockdown K562 cells as compared with the vector control cells. However, the mRNA expression of CXCR1 was not altered in these cells. We next examined the effect of STAP-2 on SDF-1α-induced Ba/F3 migration. As shown in Figure 8c, there was a reduction in migration in the BCL-ABL-expressing Ba/F3 cells in response to SDF-1α, although spontaneous migration was slightly enhanced in the BCL-ABL-expressing Ba/F3 cells. There was enhanced migration in the STAP-2-expressing Ba/F3 cells in response to SDF-1α corresponding to the fact that STAP-2 enhanced SDF-1α-induced cell migration in Jurkat T-cells. Importantly, a significant reduction of SDF-1α-induced cell migration was observed in the BCR-ABL/STAP-2-expressing Ba/F3 cells as compared with the Ba/F3 cells expressing BCR-ABL alone. Therefore, STAP-2 suppresses SDF-1α-induced cell migration in BCL-ABL expressing cells by synergistically decreasing CXCR4 expression.

Discussion

In this study we demonstrated that STAP-2 interacts with, and modifies the function, of various signaling or transcription molecules (Minoguchi et al 2003, Sekine et al 2005, Sekine et al 2006, Sekine et al 2007b, Sekine et al 2009a, Yamamoto et al 2003). We also demonstrated that BCR-ABL acts as a novel binding partner for STAP-2 in the presence of both the STAP-2 SH2-like domain and STAP-2 Tyr250 phosphorylation. Importantly, STAP-2 SH2-like domain is required for physical and functional interactions between STAP-2 and BCR-ABL. The interaction between STAP-2 and BCR-ABL led to increased BCR-ABL phosphorylation status. Moreover, there was also an effect on downstream signaling resulting in the enhanced cell proliferation and the altered chemokine receptor expression. An important finding of this study was that STAP-2 cooperates with BCR-ABL to change tumor progression patterns in mice injected with transfected Ba/F3 cells. Furthermore, suppression of STAP-2 in human K562 CML cells resulted in no tumor formation in mice. Therefore, STAP-2 is likely to be involved in the pathogenesis of CML.

In general, BCR-ABL activates multiple signaling pathways, which induce cell growth and survival (Quintas-Cardama and Cortes 2009, Ren 2005). The RAS-MAPK pathway is activated leading to the induction of Bcl-2 transcription. The PI3 kinase-AKT pathway is also activated and mediates a network of targets, including FoxO proteins, Bad, glycogen synthase kinase 3β (Brunet et al 1999, Datta et al 1997, del Peso et al 1997, Pap and Cooper 1998). This BCR-ABL-dependent PI3 kinase activation is in part mediated by Gab2 and/or c-Cbl (Chu et al 2007, Sattler et al 1996). Further, STAT5, which regulates cyclin D1 and Bcl-xL, is activated by BCR-ABL independent of Jak family proteins (Xie et al 2001). STAT5a/b-deficient fetal liver hematopoietic progenitors fail to generate leukemia in recipient mice after retroviral transduction with BCR-ABL (Hoelbl et al 2006). Among these BCR-ABL-related signaling molecules, we previously found that STAP-2 binds to and regulates c-Cbl and STAT5 (Sekine et al 2005, Sekine et al 2009b). In particular, in a breast cancer model, STAP-2 was found to greatly enhance BRK-mediated STAT5 activation (Ikeda et al 2011, Sekine et al

2007b). Therefore, in addition to increased BCR-ABL phosphorylation, STAP-2 is likely to be involved in multiple events downstream of BCR-ABL. In this study, BCR-ABL-mediated expression of BCL-2 and BCL-xL was largely depending on the level of STAP-2. Manipulation of STAP-2 expression altered phosphorylation state of various signaling molecules. Among them, ERK phosphorylation well correlated to expression levels of BCL-2 and BCL-xL. Because the BCR-ABL - Ras pathway is one of major signals, the two anti-apoptotic molecules may be controlled by STAP-2 in BCR-ABL-positive cells. Alternatively, STAT5, another signaling molecule to drive expression of BCL-2 and BCL-xL may also participate in this process. We showed that STAT5 expression level was influenced by the interaction between BCR-ABL and STAP-2.

Resistance to imatinib in CML patients has been related to changes to BCR-ABL-dependent or independent mechanisms (Quintas-Cardama and Cortes 2009). The most frequent process underlying this mechanism is point mutations to BCR-ABL involving the ATP-binding pocket, which prevent imatinib binding (Hughes et al 2006, O'Hare et al 2007). However, other mechanisms have also been implicated including the duplication and amplification of the BCR-ABL (le Coutre et al 2000, Weisberg and Griffin 2000). Imatinib export via the p-glycoprotein efflux pump (Mahon et al 2000), reduced expression of the organic cation transporter OCT1 (Crossman et al 2005, Wang et al 2008), binding of imatinib to the plasma by α1-acid glycoprotein (Gambacorti-Passerini et al 2003a) and the activation of alternative signaling cascades leading to BCR-ABL-independent growth (Donato et al 2003, Ptasznik et al 2004). With regard to STAP-2 expression, one gene expression database on CML patient samples reported that STAP-2 was expressed by $CD34^+$ cells (Bruennert D 2009). Our data also indicate that STAP-2 plays a role in acquiring resistance to imatinib through alternative pathways, including enhancing BCR-ABL activity. A putative mechanism is that binding of STAP-2 induces conformational change of BCR-ABL, increasing its affinity to ATP. Another potential mechanism is that STAT-2 modifies the interaction between BCR-ABL and imatinib. However, further analysis is required to clarify the relationship between STAP-2, BCR-ABL and imatinib, and the potential to utilize STAP-2 expression in the

prediction of imatinib sensitivity.

The CXCR4 chemokine receptor belongs to a family of seven transmembrane-spanning proteins. The natural ligand for CXCR4 is SDF-1α, a CXC chemokine constitutively produced by bone marrow stromal cells. Inhibition of CXCR4 function via blocking antibodies results in a considerable delay in bone marrow engraftment by human hematopoietic stem cells into NOD-SCID mice (Peled et al 1999), coupled with the appearance of CXCR4-deficient hematopoietic progenitors in the circulation (Ma et al 1999). Thus, the expression of CXCR4 on hematopoietic stem/progenitor cells is involved in their homing and retention in bone marrow. Several studies have reported cross-talk between BCR-ABL and CXCR4. In hematopoietic cell lines, overexpression of BCR-ABL revealed impaired migration and signaling in response to SDF-1α (Salgia et al 1999). Further, BCR-ABL, depending on its level of expression, also diminishes CXCR4 expression at the level of transcription (Geay et al 2005). Moreover, the treatment of CML-derived cell lines with BCR-ABL inhibitors increased the expression of CXCR4 and migration to SDF-1α (Jin et al 2008). Collectively, the downregulation of CXCR4 by BCR-ABL seems to be a powerful explanation as to why premature myeloid cells migrate away from the bone marrow in CML. In this study we demonstrated that CXCR4 expression was dramatically reduced when both STAP-2 and BCR-ABL were simultaneously transfected into Ba/F3 cells, which express neither STAP2 nor BCR-ABL. In K562 cells, which express both STAP-2 and BCR-ABL, CXCR4 expression was greatly enhanced by the inhibition of STAP-2. Thus, our data suggest a strong involvement of STAP-2 in the linkage of BCR-ABL and CXCR4. Coupled with our previous results indicating that STAP-2 suppresses SDF-1α signaling through interactions with Vav (Sekine et al 2009a), STAP-2 is likely to regulate SDF-1α/CXCR4 at multiple levels in CML cells. Therefore, STAP-2 is likely to play a crucial role in the pathogenesis of CML.

The differences in tumor progression observed between BCR-ABL and BCR-ABL/STAP-2-expressing Ba/F3 cells represent an attractive target for the development of

therapies for CML. A massive infiltration of tumor cells into the lymph nodes, spleen and liver was observed when Ba/F3 cells expressing BCR-ABL/STAP-2, but not BCR-ABL were implanted into mice. Our data regarding chemokine receptors may explain this difference. In addition to CXCR4 expression, STAP-2 may interact with BCR-ABL to upregulate CCR1 and CCR7 expression. Because CCR7 interacts with secondary lymphoid tissue chemokines such as CCL19 and CCL21 (Mburu et al 2006), such a change of chemokine receptor expression may in part explain the different invasiveness. It would be of interest to determine whether the chemokine receptor expression profile, depending on STAP-2 expression, may be related to the splenomegaly observed in CML patients.

In summary, this study provides evidence that STAP-2 is significantly involved in BCR-ABL activation and that STAP-2 expression plays a crucial role in the BCR-ABL-mediated growth advantage, altered chemokine receptor expression and the resistance to imatinib. Therefore, STAP-2 is likely to underlie CML progression and imatinib-sensitivity. Collectively, STAP-2 is essential for the complete activation of BCR-ABL in CML cells. Thus, STAP-2 represents a suitable molecular target against which novel strategies to treat CML might be developed and STAP-2 expression has the potential to offer useful insight into the characteristics of individual CML clones.

Materials and methods

Reagents and antibodies

Recombinant human SDF-1α was purchased from PeproTech (London, UK). BCR-ABL tyrosine kinase inhibitor STI571, imatinib mesylate, was kindly gifted by Novartis Pharmaceuticals (Basel, Switzerland). Expression vectors for p190/p210BCR-ABL, ABL, STAP-2 and their mutants were described previously (Minoguchi et al 2003, Sekine et al 2005, Tokunaga et al 2010, Toyofuku et al 2004). Expression vectors for Myc-tagged-BCR was generated by PCR methods and sequenced (primer sequences are available upon request). Anti-ABL anti-BCL-2, anti-BCL-xL, and anti-phospho ERK (pERK) antibodies were obtained from Santa Cruz Biotechnology (Santa Cruz, CA, USA). Anti-Myc, anti-GST, anti-actin mAb and anti-phosphotyrosine (PY) mAb (PY20) were purchased from Sigma-Aldrich (St. Louis, MO, USA). Anti-ERK antibody was purchased from Cell signaling Technologies (Beverly, MA). Anti-VAV antibody was purchased from Millipore (Billerica, MA). Anti-CBL antibody was purchased from Epitomics, Inc. (Burlingame, CA). Anti-STAP-2 antibody was purchased from Everest Biotech (Oxfordshire, UK). Anti-phophoSTAP-2 Tyr250 antibody was prepared as previously described (Sekine et al 2007a).

Cell culture and establishment of cell lines

Human embryonic kidney carcinoma cell line, 293T was maintained in Dulbecco's modified Eagle's medium (DMEM) containing 10% fetal calf serum (FCS) and transfected by the standard calcium precipitation protocol. Interleukin (IL)-3-dependent murine pro-B cell line, Ba/F3 was maintained in RPMI1640 medium supplemented with 10% FCS with 10% of WEHI-3B conditioned medium as a source of IL-3 (Sekine et al 2005). Stable Ba/F3 transformants expressing pcDNA3 (Ba/F3-pcDNA), pcDNA3-STAP-2 (Ba/F3-STAP-2) or pcDNA3-p210BCR-ABL (Ba/F3-p210) were established by transfection of with pcDNA3-vector, pcDNA3-STAP-2 and pcDNA3-p210BCR-ABL, and then selected with G418 (0.5 mg/mL; Sigma-Aldrich) as described

previously (Sekine et al 2005). Stable Ba/F3 transformants expressing both pcDNA3-p210BCR-ABL and pcDNA3-STAP-2 (Ba/F3-p210/STAP-2) were established by transfection of with pcDNA3-STAP-2 or pcDNA3.1/Hygro vector into Ba/F3-p210 cells and then selected with Hygromycin (0.2 mg/mL). Similarly, Ba/F3-p210/STAP-2 Y250F (#1 and #2) and Ba/F3-p210/STAP-2 ΔSH2 (#1 and #2) cells were also established as described the above. Human leukemic cell lines, K562 were maintained in RPMI1640 medium supplemented with 10% FCS. Stable STAP-2 knockdown K562 cell lines (K562-shSTAP-2 #1 and #2) were established by transfection of with pGPU6/GFP/Neo vector (Shanghai GenePharm , Shanghai, China) bearing short hairpin RNA (shRNA) targeting STAP-2 (#1; 5'-CCAGCTGTTGACTATGAGA-3' , #2; 5'-CCAGTCATCCTGAAGCCAA-3') and then selected with G418 (0.5 mg/mL). Similarly, control shRNA (non-sliencing; 5'- TTCTCCGAACGTGTCACGT-3')-transfected K562 cell lines (K562-shControl #1 and #2) were also established.

Conflict of interest

The authors have no conflicting financial interests.

Acknowledgements

This study was supported in part by the Grant-in-Aid for scientific research from Ministry of Education, Culture, Sports, Science and Technology of Japan.

References

Brehme M, Hantschel O, Colinge J, Kaupe I, Planyavsky M, Kocher T *et al* (2009). Charting the molecular network of the drug target Bcr-Abl. *Proc Natl Acad Sci U S A* **106:** 7414-7419.

Brunet A, Bonni A, Zigmond MJ, Lin MZ, Juo P, Hu LS *et al* (1999). Akt promotes cell survival by phosphorylating and inhibiting a Forkhead transcription factor. *Cell* **96:** 857-868.

Chang YC, Tien SC, Tien HF, Zhang H, Bokoch GM, Chang ZF (2009). p210(Bcr-Abl) desensitizes Cdc42 GTPase signaling for SDF-1alpha-directed migration in chronic myeloid leukemia cells. *Oncogene* **28:** 4105-4115.

Chu S, Li L, Singh H, Bhatia R (2007). BCR-tyrosine 177 plays an essential role in Ras and Akt activation and in human hematopoietic progenitor transformation in chronic myelogenous leukemia. *Cancer Res* **67:** 7045-7053.

Corbin AS, La Rosee P, Stoffregen EP, Druker BJ, Deininger MW (2003). Several Bcr-Abl kinase domain mutants associated with imatinib mesylate resistance remain sensitive to imatinib. *Blood* **101:** 4611-4614.

Cortes J, Jabbour E, Kantarjian H, Yin CC, Shan J, O'Brien S *et al* (2007). Dynamics of BCR-ABL kinase domain mutations in chronic myeloid leukemia after sequential treatment with multiple tyrosine kinase inhibitors. *Blood* **110:** 4005-4011.

Crossman LC, Druker BJ, Deininger MW, Pirmohamed M, Wang L, Clark RE (2005). hOCT 1 and resistance to imatinib. *Blood* **106:** 1133-1134; author reply 1134.

Datta SR, Dudek H, Tao X, Masters S, Fu H, Gotoh Y *et al* (1997). Akt phosphorylation of BAD couples survival signals to the cell-intrinsic death machinery. *Cell* **91:** 231-241.

del Peso L, Gonzalez-Garcia M, Page C, Herrera R, Nunez G (1997). Interleukin-3-induced phosphorylation of BAD through the protein kinase Akt. *Science* **278:** 687-689.

Donato NJ, Wu JY, Stapley J, Gallick G, Lin H, Arlinghaus R *et al* (2003). BCR-ABL independence and LYN kinase overexpression in chronic myelogenous leukemia cells selected for resistance to STI571. *Blood* **101:** 690-698.

Gambacorti-Passerini C, Zucchetti M, Russo D, Frapolli R, Verga M, Bungaro S *et al* (2003a). Alpha1 acid glycoprotein binds to imatinib (STI571) and substantially alters its pharmacokinetics in chronic myeloid leukemia patients. *Clin Cancer Res* **9:** 625-632.

Gambacorti-Passerini CB, Gunby RH, Piazza R, Galietta A, Rostagno R, Scapozza L (2003b). Molecular mechanisms of resistance to imatinib in Philadelphia-chromosome-positive leukaemias. *Lancet Oncol* **4:** 75-85.

Geay JF, Buet D, Zhang Y, Foudi A, Jarrier P, Berthebaud M *et al* (2005). p210BCR-ABL inhibits SDF-1 chemotactic response via alteration of CXCR4 signaling and down-regulation of CXCR4 expression. *Cancer Res* **65:** 2676-2683.

Gorre ME, Mohammed M, Ellwood K, Hsu N, Paquette R, Rao PN *et al* (2001). Clinical resistance to STI-571 cancer therapy caused by BCR-ABL gene mutation or amplification. *Science* **293:** 876-880.

Hochhaus A, La Rosee P (2004). Imatinib therapy in chronic myelogenous leukemia: strategies to avoid and overcome resistance. *Leukemia* **18:** 1321-1331.

Hoelbl A, Kovacic B, Kerenyi MA, Simma O, Warsch W, Cui Y *et al* (2006). Clarifying the role of Stat5 in lymphoid development and Abelson-induced transformation. *Blood* **107:** 4898-4906.

Hughes T, Deininger M, Hochhaus A, Branford S, Radich J, Kaeda J *et al* (2006). Monitoring CML patients responding to treatment with tyrosine kinase inhibitors: review and recommendations for harmonizing current methodology for detecting BCR-ABL transcripts and kinase domain mutations and for expressing results. *Blood* **108:** 28-37.

Ikeda O, Mizushima A, Sekine Y, Yamamoto C, Muromoto R, Nanbo A *et al* (2011). Involvement of STAP-2 in Brk-mediated phosphorylation and activation of STAT5 in breast cancer cells. *Cancer Sci* **102:** 756-761.

Jin L, Tabe Y, Konoplev S, Xu Y, Leysath CE, Lu H *et al* (2008). CXCR4 up-regulation by imatinib induces chronic myelogenous leukemia (CML) cell migration to bone marrow stroma and promotes survival of quiescent CML cells. *Mol Cancer Ther* **7:** 48-58.

le Coutre P, Tassi E, Varella-Garcia M, Barni R, Mologni L, Cabrita G *et al* (2000). Induction of resistance to the Abelson inhibitor STI571 in human leukemic cells through gene amplification. *Blood* **95:** 1758-1766.

Lowenberg B (2003). Minimal residual disease in chronic myeloid leukemia. *N Engl J Med* **349:** 1399-1401.

Ma Q, Jones D, Springer TA (1999). The chemokine receptor CXCR4 is required for the retention

of B lineage and granulocytic precursors within the bone marrow microenvironment. *Immunity* **10:** 463-471.

Mahon FX, Deininger MW, Schultheis B, Chabrol J, Reiffers J, Goldman JM *et al* (2000). Selection and characterization of BCR-ABL positive cell lines with differential sensitivity to the tyrosine kinase inhibitor STI571: diverse mechanisms of resistance. *Blood* **96:** 1070-1079.

Mahon FX, Rea D, Guilhot J, Guilhot F, Huguet F, Nicolini F *et al* (2010). Discontinuation of imatinib in patients with chronic myeloid leukaemia who have maintained complete molecular remission for at least 2 years: the prospective, multicentre Stop Imatinib (STIM) trial. *Lancet Oncol* **11:** 1029-1035.

Mburu YK, Wang J, Wood MA, Walker WH, Ferris RL (2006). CCR7 mediates inflammation-associated tumor progression. *Immunol Res* **36:** 61-72.

Minoguchi M, Minoguchi S, Aki D, Joo A, Yamamoto T, Yumioka T *et al* (2003). STAP-2/BKS, an adaptor/docking protein, modulates STAT3 activation in acute-phase response through its YXXQ motif. *J Biol Chem* **278:** 11182-11189.

Mitchell PJ, Sara EA, Crompton MR (2000). A novel adaptor-like protein which is a substrate for the non-receptor tyrosine kinase, BRK. *Oncogene* **19:** 4273-4282.

O'Hare T, Eide CA, Deininger MW (2007). Bcr-Abl kinase domain mutations, drug resistance, and the road to a cure for chronic myeloid leukemia. *Blood* **110:** 2242-2249.

Pap M, Cooper GM (1998). Role of glycogen synthase kinase-3 in the phosphatidylinositol 3-Kinase/Akt cell survival pathway. *J Biol Chem* **273:** 19929-19932.

Peled A, Petit I, Kollet O, Magid M, Ponomaryov T, Byk T *et al* (1999). Dependence of human stem cell engraftment and repopulation of NOD/SCID mice on CXCR4. *Science* **283:** 845-848.

Pendergast AM, Muller AJ, Havlik MH, Maru Y, Witte ON (1991). BCR sequences essential for transformation by the BCR-ABL oncogene bind to the ABL SH2 regulatory domain in a non-phosphotyrosine-dependent manner. *Cell* **66:** 161-171.

Ptasznik A, Nakata Y, Kalota A, Emerson SG, Gewirtz AM (2004). Short interfering RNA (siRNA) targeting the Lyn kinase induces apoptosis in primary, and drug-resistant, BCR-ABL1(+) leukemia cells. *Nat Med* **10:** 1187-1189.

Quintas-Cardama A, Cortes J (2009). Molecular biology of bcr-abl1-positive chronic myeloid

leukemia. *Blood* **113:** 1619-1630.

Ren R (2005). Mechanisms of BCR-ABL in the pathogenesis of chronic myelogenous leukaemia. *Nat Rev Cancer* **5:** 172-183.

Salgia R, Quackenbush E, Lin J, Souchkova N, Sattler M, Ewaniuk DS *et al* (1999). The BCR/ABL oncogene alters the chemotactic response to stromal-derived factor-1alpha. *Blood* **94:** 4233-4246.

Sattler M, Salgia R, Okuda K, Uemura N, Durstin MA, Pisick E *et al* (1996). The proto-oncogene product p120CBL and the adaptor proteins CRKL and c-CRK link c-ABL, p190BCR/ABL and p210BCR/ABL to the phosphatidylinositol-3' kinase pathway. *Oncogene* **12:** 839-846.

Sekine Y, Yamamoto T, Yumioka T, Sugiyama K, Tsuji S, Oritani K *et al* (2005). Physical and functional interactions between STAP-2/BKS and STAT5. *J Biol Chem* **280:** 8188-8196.

Sekine Y, Yumioka T, Yamamoto T, Muromoto R, Imoto S, Sugiyma K *et al* (2006). Modulation of TLR4 signaling by a novel adaptor protein signal-transducing adaptor protein-2 in macrophages. *J Immunol* **176:** 380-389.

Sekine Y, Tsuji S, Ikeda O, Kakisaka M, Sugiyama K, Yoshimura A *et al* (2007a). Leukemia inhibitory factor-induced phosphorylation of STAP-2 on tyrosine-250 is involved in its STAT3-enhancing activity. *Biochem Biophys Res Commun* **356:** 517-522.

Sekine Y, Tsuji S, Ikeda O, Sugiyma K, Oritani K, Shimoda K *et al* (2007b). Signal-transducing adaptor protein-2 regulates integrin-mediated T cell adhesion through protein degradation of focal adhesion kinase. *J Immunol* **179:** 2397-2407.

Sekine Y, Ikeda O, Tsuji S, Yamamoto C, Muromoto R, Nanbo A *et al* (2009a). Signal-transducing adaptor protein-2 regulates stromal cell-derived factor-1 alpha-induced chemotaxis in T cells. *J Immunol* **183:** 7966-7974.

Sekine Y, Yamamoto C, Ikeda O, Muromoto R, Nanbo A, Oritani K *et al* (2009b). The protein content of an adaptor protein, STAP-2 is controlled by E3 ubiquitin ligase Cbl. *Biochem Biophys Res Commun* **384:** 187-192.

Shah NP, Nicoll JM, Nagar B, Gorre ME, Paquette RL, Kuriyan J *et al* (2002). Multiple BCR-ABL kinase domain mutations confer polyclonal resistance to the tyrosine kinase inhibitor imatinib (STI571) in chronic phase and blast crisis chronic myeloid leukemia. *Cancer Cell* **2:** 117-125.

Tokunaga M, Ezoe S, Tanaka H, Satoh Y, Fukushima K, Matsui K *et al* (2010). BCR-ABL but not JAK2 V617F inhibits erythropoiesis through the Ras signal by inducing p21CIP1/WAF1. *J Biol Chem* **285:** 31774-31782.

Toyofuku T, Zhang H, Kumanogoh A, Takegahara N, Yabuki M, Harada K *et al* (2004). Guidance of myocardial patterning in cardiac development by Sema6D reverse signalling. *Nat Cell Biol* **6:** 1204-1211.

Wang L, Giannoudis A, Lane S, Williamson P, Pirmohamed M, Clark RE (2008). Expression of the uptake drug transporter hOCT1 is an important clinical determinant of the response to imatinib in chronic myeloid leukemia. *Clin Pharmacol Ther* **83:** 258-264.

Weisberg E, Griffin JD (2000). Mechanism of resistance to the ABL tyrosine kinase inhibitor STI571 in BCR/ABL-transformed hematopoietic cell lines. *Blood* **95:** 3498-3505.

Xie S, Wang Y, Liu J, Sun T, Wilson MB, Smithgall TE *et al* (2001). Involvement of Jak2 tyrosine phosphorylation in Bcr-Abl transformation. *Oncogene* **20:** 6188-6195.

Yamamoto T, Yumioka T, Sekine Y, Sato N, Minoguchi M, Yoshimura A *et al* (2003). Regulation of FcepsilonRI-mediated signaling by an adaptor protein STAP-2/BSK in rat basophilic leukemia RBL-2H3 cells. *Biochem Biophys Res Commun* **306:** 767-773.

Figure legends

Figure 1 STAP-2 binds to BCR-ABL as well as BCR and ABL proteins.
(a) 293T cells ($1x10^7$) were transfected with Myc-tagged BCR (10 μg) with or without GST-fused STAP-2 (8 μg). At 48 h after transfection, the cells were lysed, and pull down with glutathione (GSH)-Sepharose and blotted with anti-Myc (upper panel) or anti-GST antibody (middle panel). An aliquot of total cell lysate (TCL) was also blotted with anti-Myc antibody (lower panel). (**b)** 293T cells ($1x10^7$) were transfected with p190/p210BCR-ABL (10 μg) with or without Myc-tagged STAP-2 (8 μg). At 48 h after transfection, the cells were lysed, and immunoprecipitated with anti-Myc antibody and blotted with anti-ABL (upper panel) or anti-Myc antibody (middle panel). An aliquot of TCL was also blotted with anti-ABL antibody (lower panel). (**c)** 293T cells ($1x10^7$) were transfected with Myc-tagged STAP-2 (10 μg) with or without His-ABL (10 μg). At 48 h after transfection, the cells were lysed, and immunoprecipitated with anti-ABL antibody and blotted with anti-Myc (upper panel) or anti-ABL antibody (middle panel). An aliquot of TCL was also blotted with anti-Myc antibody (lower panel). (**d)** Human leukemic cell line, K562 cells ($3x10^7$) were lysed, and immunoprecipitated with control IgG or anti-STAP-2 antibody and immunoblotted with anti-ABL (upper panel) or anti-STAP-2 (lower panel).

Figure 2 STAP-2 enhances BCR-ABL activity in Ba/F3 cells.
(a) Ba/F3-p210 and Ba/F3-p210/STAP-2 (#1 and #2) cells ($3x10^3$ cells/well) in 96-well plates were cultured without IL-3 (WEHI-3B conditioned medium) for the indicated periods. The cell numbers were measured using a Cell Counting Kit-8. The data are the means of triplicate experiments, which generally varied by <10%. Similar results were obtained in three independent experiments. *** indicates significant difference $p<0.001$. (vs. Ba/F3-p210) (**b)** Ba/F3-p210 and Ba/F3-p210/STAP-2 (#1 and #2) cells ($2x10^4$ cells/well) in 96-well plates were cultured without IL-3 (WEHI-3B conditioned medium) in the presence of STI571 (0, 1, 3, 5 μM) for 24 hrs. The cell numbers were measured using a Cell Counting Kit-8. The data are the means of triplicate

experiments, which generally varied by <10%. Similar results were obtained in three independent experiments. * and *** indicate significant difference $p<0.05$ and $p<0.001$, respectively. (vs. Ba/F3-p210) (**c)** Ba/F3-p210 and Ba/F3-p210/STAP-2 (#1 and #2) cells ($1x10^6$ cells/well) in 12-well plates were cultured with or without IL-3 (5% of WEHI-3B conditioned medium) for 24 hrs. The cells were lysed, and immunobloted with anti-PY, anti-ABL, anti-Myc, anti-pERK, anti-ERK, anti-Bcl-xL, anti-Bcl-2, and anti-Actin antibody. (**d)** Ba/F3-p210 and Ba/F3-p210/STAP-2 (#1 and #2) cells ($1x10^6$ cells) were cultured without IL-3 (WEHI-3B conditioned medium) for 24 hrs. The cells were lysed, and immunobloted with anti-PY, anti-ABL, or anti-Myc antibody. (**e)** Ba/F3-p210 and Ba/F3-p210/STAP-2 (#1 and #2) cells ($1x10^7$ cells) were cultured without IL-3 (WEHI-3B conditioned medium) for 24 hrs. The cells were lysed, and immunoprecipitated with anti-STAT5b antibody and immunobloted with anti-PY, or anti-STAT5b antibody. (**f)** Ba/F3-p210 and Ba/F3-p210/STAP-2 (#1 and #2) cells were cultured without IL-3 (WEHI-3B conditioned medium) for 24 hrs. The cells were then fixed and stained with propidium iodide (PI). The DNA content of nuclei was analyzed using FACS Calibur and CellQuest software.

Figure 3 STAP-2 enhances BCR-ABL activity in K562 cells.

(a) K562-shControl(#1 and #2) and K562-shSTAP-2 (#1and #2) cells were established. Total RNA samples isolated from these cells were also quantified by reverse transcription and quantitative real-time PCR analysis. Data represent the levels of these mRNA normalized to that of an *ACTIN* internal control and are expressed relative to the value of control siRNA-treated samples. Shown is a representative experiment, which was repeated at least three times with similar results. (**b)** K562-shControl(#1 and #2) and K562-shSTAP-2 (#1and #2) cells ($5x10^3$ cells/well) in 96-well plates were cultured for the indicated periods. Cell growth was measured using a Cell Counting Kit-8. The data are the means of triplicate experiments, which generally varied by <10%. Similar results were obtained in three independent experiments. ** and *** indicate significant difference $p<0.01$ and $p<0.001$, respectively. (vs. K562-shControl #1) (**c)** K562-shControl(#1 and #2) and

K562-shSTAP-2 (#1and #2) cells ($2x10^4$ cells/well) in 96-well plates cultured in the presence of STI571 (0, 3, 5, 10 μM) in 96-well plates for 24 hrs. Cell growth was measured using a Cell Counting Kit-8. The data are the means of triplicate experiments, which generally varied by <10%. Similar results were obtained in three independent experiments. * and ** indicate significant difference $p<0.05$ and $p<0.01$, respectively. (vs. K562-shControl #1) (**d, e).** K562-shControl(#1 and #2) and K562-shSTAP-2 (#1and #2) cells ($1x10^6$ cells/well) in 12-well plates were cultured for 24 hrs. The cells were lysed, and immunobloted with anti-PY described in **d**, anti-pSTAT5, anti-STAT5b, anti-PY, anti-ABL, anti-pERK, anti-ERK, anti-BCL-xL and anti-Actin antibody described in **e**. (**f)** K562-shControl(#1 and #2) and K562-shSTAP-2 (#1and #2) cells ($5x10^6$ cells) cells were lysed, and immunoprecipitated with anti-CBL (upper panels) or anti-VAV antibody (lower panels) and blotted with anti-PY, anti-CBL or anti-VAV antibody. An aliquot of TCL was also blotted with anti-CBL or anti-VAV antibody. (**g)** Total RNA samples isolated from K562-shControl (#1 and #2) and K562-shSTAP-2 (#1 and #2) cells were subjected to RT-PCR analysis using STAT5b, BCL-2, BCL-xL, CYCLIN D1 and G3PDH primers. *, ** and *** indicate significant difference $p<0.05$, $p<0.01$ and $p<0.001$, respectively.

Figure 4 The SH2 domain of STAP-2 binds to BCR-ABL.

(a) Schematic diagrams of the domain structures of the GST-fused STAP-2 mutant fragments. (**b)** 293T cells ($1x10^7$) were transfected with p210BCR-ABL (10 μg) with or without GST-fused STAP-2 mutants (8 μg). At 48 h after transfection, the cells were lysed, and pull down with GSH-Sepharose and immunoblotted with an anti-PY, anti-ABL and anti-GST antibody. An aliquot of each total cell lysate (TCL) was immunoblotted with anti-PY or anti-ABL antibody. (**c)** Ba/F3-p210, Ba/F3-p210/STAP-2#2 and Ba/F3-p210/STAP-2 ΔSH2 (#1and #2) cells ($3x10^3$ cells/well) in 96-well plates were cultured without IL-3 (WEHI-3B conditioned medium) for the indicated periods. Cell growth was using a Cell Counting Kit-8. The data are the means of triplicate experiments, which generally varied by <10%. Similar results were obtained in three independent

experiments. *** indicates significant difference $p<0.001$. (vs. Ba/F3-p210/STAP-2WT#2) **(d)** Ba/F3-p210, Ba/F3-p210/STAP-2#2 and Ba/F3-p210/STAP-2 ΔSH2 (#1 and #2) cells ($2x10^4$ cells/well) in 96-well plates were cultured without IL-3 (WEHI-3B conditioned medium) in the presence of STI571 (0, 1, 3, 5 μM) for 24 hrs. The cell numbers were measured using a Cell Counting Kit-8. The data are the means of triplicate experiments, which generally varied by <10%. Similar results were obtained in three independent experiments. ** and *** indicate significant difference $p<0.01$ and $p<0.001$, respectively. (vs. Ba/F3-p210/STAP-2WT#2) **(e)** Ba/F3-p210, Ba/F3-p210/STAP-2#2 and Ba/F3-p210/STAP-2 ΔSH2 (#1 and #2) cells ($1x10^6$ cells/well) in 12-well plates were cultured with or without IL-3 (5% of WEHI-3B conditioned medium) for 24 hrs. The cells were lysed, and immunobloted with anti-PY, anti-ABL, anti-Myc, anti-pERK, anti-ERK, anti-BCL-xL, anti-BCL-2 and anti-Actin antibody. **(f)** Ba/F3-p210, Ba/F3-p210/STAP-2#2 and Ba/F3-p210/STAP-2 ΔSH2 (#1 and #2) cells ($1x10^6$ cells) were cultured with or without IL-3 (5% of WEHI-3B conditioned medium) for 24 hrs. The cells were lysed, and immunobloted with anti-PY, anti-ABL or anti-Myc antibody. (**g)** Ba/F3-p210, Ba/F3-p210/STAP-2#2 and Ba/F3-p210/STAP-2 ΔSH2#1 cells ($1x10^7$ cells) were lysed, and immunoprecipitated with anti-Myc antibody and immunoblotted with anti-ABL or anti-Myc (upper panels). An aliquot of TCL was also blotted with anti-ABL or anti-Myc antibody (lower panels).

Figure 5 Role of STAP-2 Tyr250 in interactions between STAP-2 and BCR-ABL

(a, b) 293T cells in a 12-well plate were transfected with Myc-tagged STAP-2 WT (1 μg) and/or p190/p210 BCR-ABL (1 μg). 48 hours after transfection, the cells were lysed. An aliquot of each total cell lysates (TCL) was immunoblotted with an anti-PY, anti-Myc or anti-ABL antibody. (**c)** Domain structure of STAP-2 is schematically shown. Four predicted tyrosine residues are also shown. (**d, e)** 293T cells in a 12-well plate were transfected with Myc-tagged STAP-2 WT (1 μg) or STAP-2 YF mutants (1 μg) and/or p190/p210BCR-ABL (1 μg). 48 hours after transfection, the

cells were lysed. An aliquot of each total cell lysates (TCL) was immunoblotted with an anti-PY, anti-pSTAP-2 Tyr250, anti-Myc or anti-ABL antibody. (**f)** Ba/F3-p210, Ba/F3-p210/STAP-2#2 and Ba/F3-p210/STAP-2 Y250F (#1 and #2) cells ($3x10^3$ cells/well) in 96-well plates were cultured without IL-3 (WEHI-3B conditioned medium) for the indicated periods. Cell growth was measured using a Cell Counting Kit-8. The data are the means of triplicate experiments, which generally varied by <10%. Similar results were obtained in three independent experiments. ** and *** indicate significant difference $p<0.01$ and $p<0.001$, respectively. (vs. Ba/F3-p210/STAP-2WT#2) (**g)** Ba/F3-p210, Ba/F3-p210/STAP-2#2 and Ba/F3-p210/STAP-2 Y250F (#1 and #2) cells ($2x10^4$ cells/well) in 96-well plates were cultured without IL-3 (WEHI-3B conditioned medium) in the presence of STI571 (0, 1, 3, 5 μM) for 24 hrs. The cell numbers were measured using a Cell Counting Kit-8. The data are the means of triplicate experiments, which generally varied by <10%. Similar results were obtained in three independent experiments. ** and *** indicate significant difference $p<0.01$ and $p<0.001$, respectively. (vs. Ba/F3-p210/STAP-2WT#2) (**h)** Ba/F3-p210, Ba/F3-p210/STAP-2#2 and Ba/F3-p210/STAP-2 Y250F (#1 and #2) cells ($1x10^6$ cells/well) in 12-well plates were cultured with or without IL-3 (5% of WEHI-3B conditioned medium) for 24 hrs. The cells were lysed, and immunobloted with anti-PY, anti-ABL, anti-Myc, anti-pERK, anti-ERK, anti-BCL-xL, anti-BCL-2 and anti-Actin antibody. (**i)** Ba/F3-p210, Ba/F3-p210/STAP-2#2 and Ba/F3-p210/STAP-2 Y250F (#1 and #2) cells ($1x10^6$ cells) were cultured with or without IL-3 (5% of WEHI-3B conditioned medium) for 24 hrs. The cells were lysed, and immunobloted with anti-PY, anti-ABL or anti-Myc antibody.

Figure 6 Different pattern of tumor progression between BCR-ABL- and BCR-ABL/STAP-2-expressing Ba/F3 cells.

Ba/F3-pcDNA, Ba/F3-p210 and Ba/F3-p210/STAP-2#2 cells were subcutaneously injected into nude mice (n=5). (**a)** For 50 days after inoculation, mouse survival was monitored daily. (**b)** Nude mice were photographed 4 weeks postinoculation with Ba/F3 cells. Arrows indicate location of

tumor. (**c, d)** 4 weeks postinoculation with Ba/F3 cells, mice were sacrificed, and the morphological changes of tumor described in **c**, liver, spleen, and lymph node described in **d** were photographed. (**e)** 4 weeks postinoculation, tumor, liver, spleen, and lymph node were weighed and graphed. *, ** and *** indicate significant difference $p<0.05$, $p<0.01$ and $p<0.001$, respectively. (**f)** Representative histological features of liver. H&E staining. Scale bar, 50μm.

Figure 7 Knockdown of STAP-2 in human K562 cells fails to form tumors *in vivo*.
K562-shControl #1 and K562-shSTAP-2 #1 cells were subcutaneously injected into nude mice. (K562-shControl#1, n=6; K562-shSTAP-2#1, n=7) (**a)** For 28 days after inoculation, tumor volume was monitored daily. * and ** indicate significant difference $p<0.05$ and $p<0.01$, respectively. (**b)** Nude mice were photographed 4 weeks postinoculation with K562 cells. Arrows indicate location of tumor. (**c)** 4 weeks postinoculation with K562 cells, mice were sacrificed, and the morphological changes of tumor described in **c** (upper panel) were photographed. Representative histological features of tumor. H&E staining. (x200 magnification and x400 magnification) (**d)** 4 weeks postinoculation, tumors were weighed and graphed.

Figure 8 STAP-2 cooperates with BCR-ABL to modify the expression of chemokine receptors
(a) Ba/F3-pcDNA, Ba/F3-STAP-2, Ba/F3-p210 and Ba/F3-p210/STAP-2#2 cells were lysed, and immunobloted with anti-PY, anti-ABL, anti-Myc and anti-Actin antibody. Total RNA samples isolated from these cells were subjected to RT-PCR analysis using CCR1, CCR7, CXCR1, CXCR4, and G3PDH primers. (**b)** Total RNA samples isolated from K562-shControl (#1 and #2) and K562-shSTAP-2 (#1 and #2) cells were subjected to RT-PCR analysis using CCR1, CCR7, CXCR1, CXCR4, STAP-2 and G3PDH primers. (**c)** The migration of Ba/F3-pcDNA, Ba/F3-STAP-2, Ba/F3-p210 and Ba/F3-p210/STAP-2#2 cells ($5x10^5$ cells) in response to SDF-1α (100 ng/mL) were studied in Transwell assay. Data are mean values of independent experiment with SDs (n =3). * and ** indicate significant difference $p<0.05$ and $p<0.01$, respectively.

Figure 1

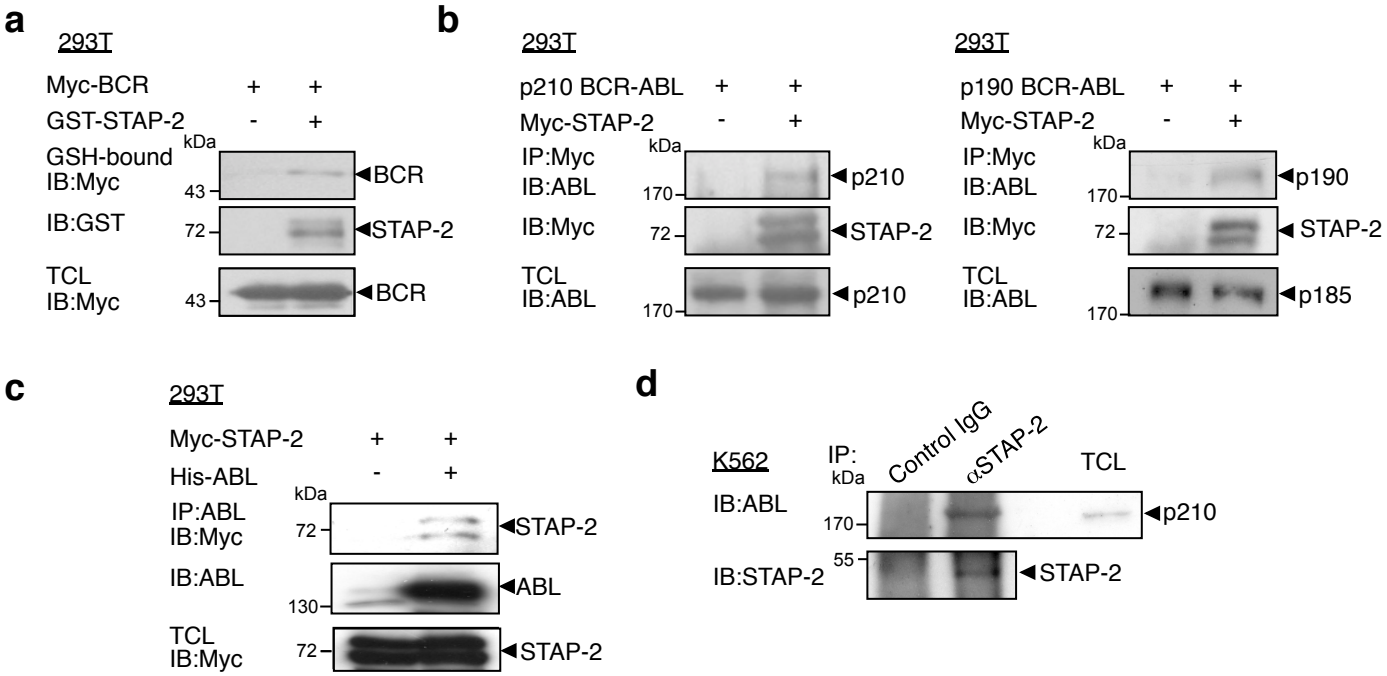
a
293T
Myc-BCR + +
GST-STAP-2 - +
GSH-bound IB:Myc
IB:GST
TCL IB:Myc
kDa
43
72
43
BCR
STAP-2
BCR
b
293T
p210 BCR-ABL + +
Myc-STAP-2 - +
IP:Myc IB:ABL
IB:Myc
TCL IB:ABL
kDa
170
72
170
p210
STAP-2
p210
293T
p190 BCR-ABL + +
Myc-STAP-2 - +
IP:Myc IB:ABL
IB:Myc
TCL IB:ABL
kDa
170
72
170
p190
STAP-2
p185
c
293T
Myc-STAP-2 + +
His-ABL - +
IP:ABL IB:Myc
IB:ABL
TCL IB:Myc
kDa
72
130
72
STAP-2
ABL
STAP-2
d
K562
IP:
kDa
Control IgG
αSTAP-2
TCL
IB:ABL
IB:STAP-2
170
55
p210
STAP-2

Figure 2

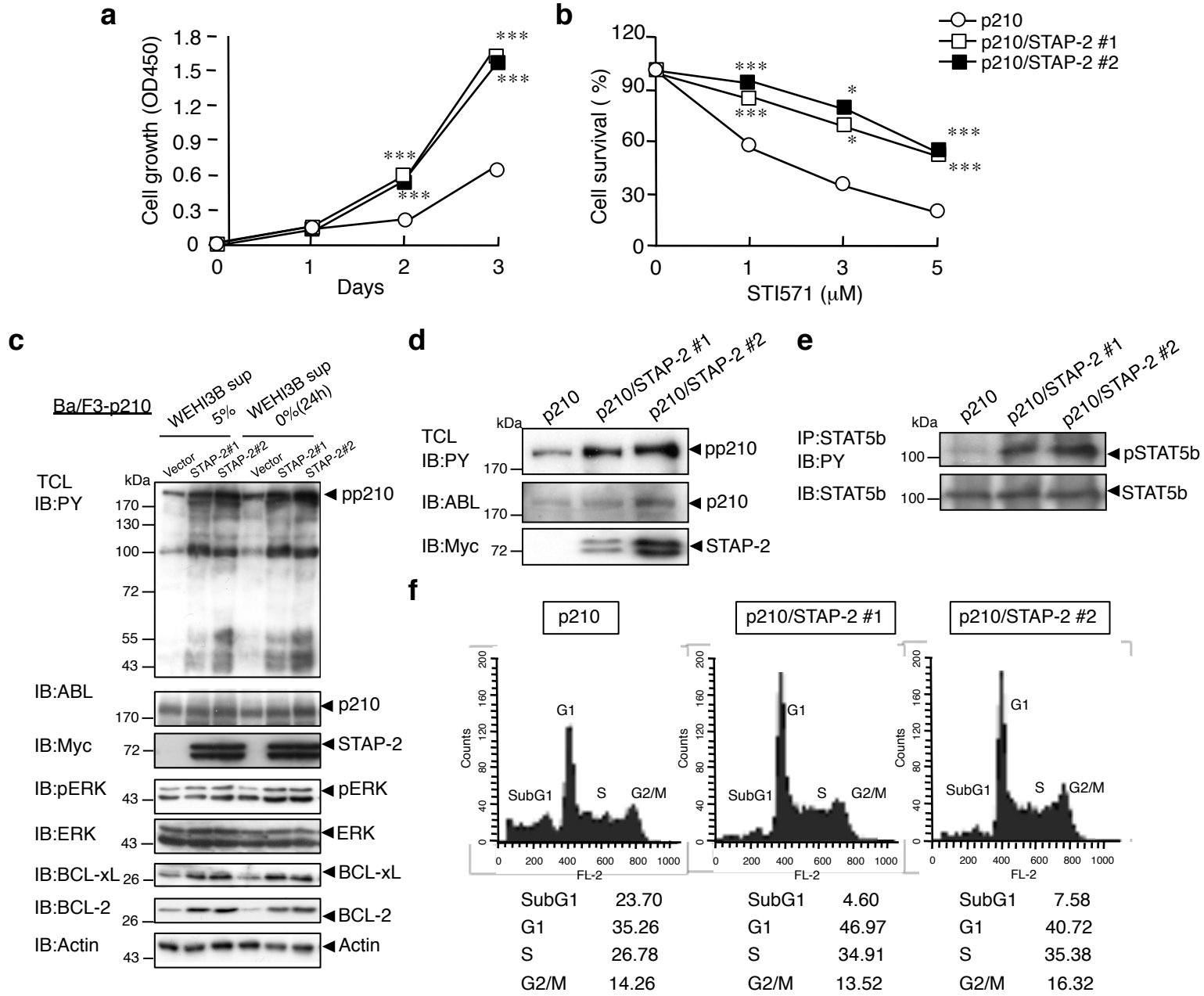
a
Cell growth (OD450)
Days
b
Cell survival (%)
STI571 (μM)
p210
p210/STAP-2 #1
p210/STAP-2 #2
c
Ba/F3-p210
WEHI3B sup 5%
WEHI3B sup 0%(24h)
Vector
STAP-2#1
STAP-2#2
TCL IB:PY
pp210
IB:ABL
p210
IB:Myc
STAP-2
IB:pERK
pERK
IB:ERK
ERK
IB:BCL-xL
BCL-xL
IB:BCL-2
BCL-2
IB:Actin
Actin
d
TCL IB:PY
IB:ABL
IB:Myc
e
IP:STAT5b IB:PY
IB:STAT5b
pSTAT5b
STAT5b
f
p210
p210/STAP-2 #1
p210/STAP-2 #2
Counts
FL-2
SubG1
G1
S
G2/M
SubG1 23.70
G1 35.26
S 26.78
G2/M 14.26
SubG1 4.60
G1 46.97
S 34.91
G2/M 13.52
SubG1 7.58
G1 40.72
S 35.38
G2/M 16.32

Figure 3

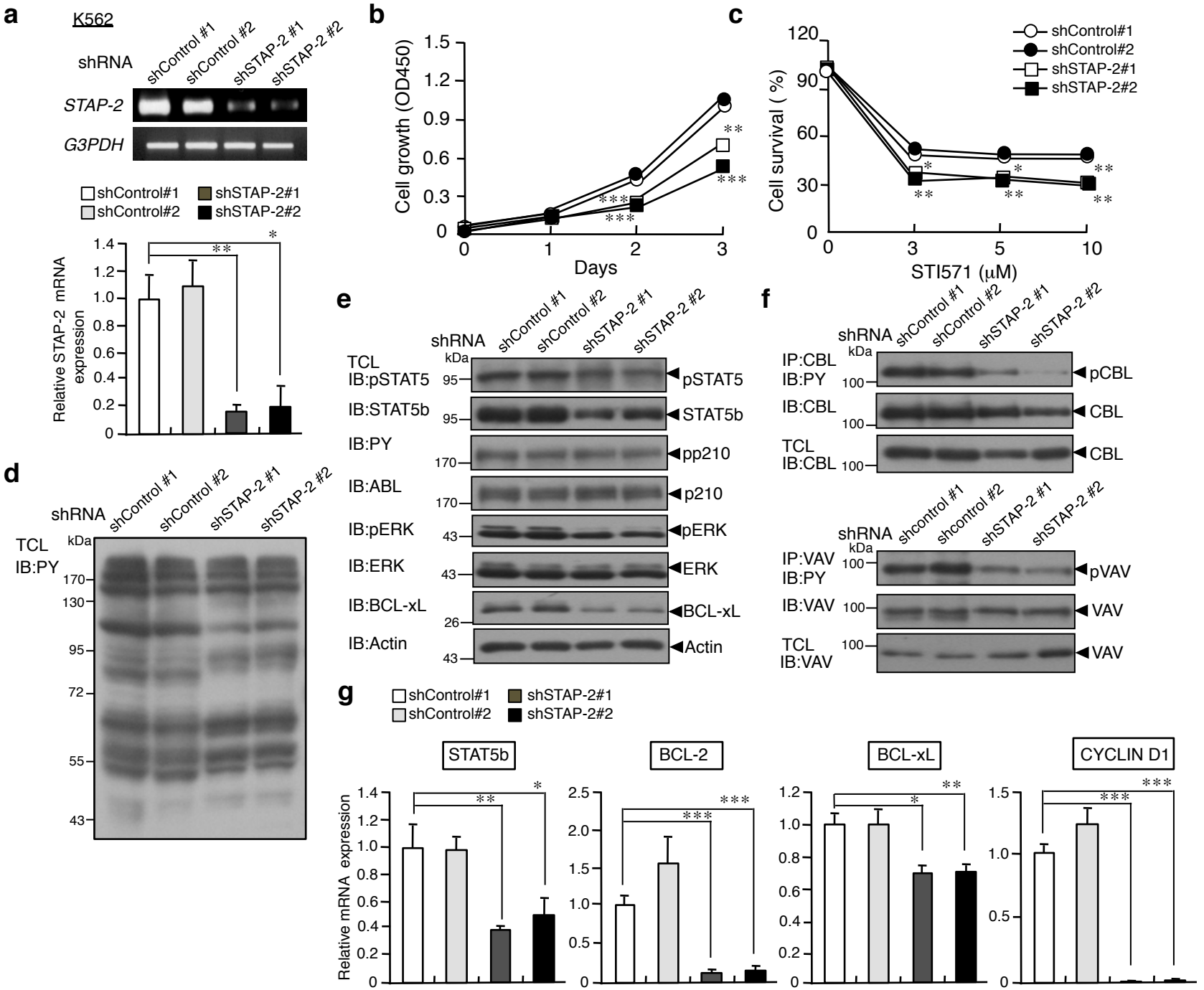
a
K562
shRNA
shControl #1
shControl #2
shSTAP-2 #1
shSTAP-2 #2
STAP-2
G3PDH
shControl#1
shControl#2
shSTAP-2#1
shSTAP-2#2
Relative STAP-2 mRNA expression
b
Cell growth (OD450)
Days
c
Cell survival (%)
STI571 (μM)
d
TCL
IB:PY
kDa
e
TCL
IB:pSTAT5
IB:STAT5b
IB:PY
IB:ABL
IB:pERK
IB:ERK
IB:BCL-xL
IB:Actin
pSTAT5
STAT5b
pp210
p210
pERK
ERK
BCL-xL
Actin
f
IP:CBL
IB:PY
IB:CBL
TCL
IB:CBL
pCBL
CBL
IP:VAV
IB:PY
IB:VAV
TCL
IB:VAV
pVAV
VAV
g
STAT5b
BCL-2
BCL-xL
CYCLIN D1
Relative mRNA expression

Figure 4

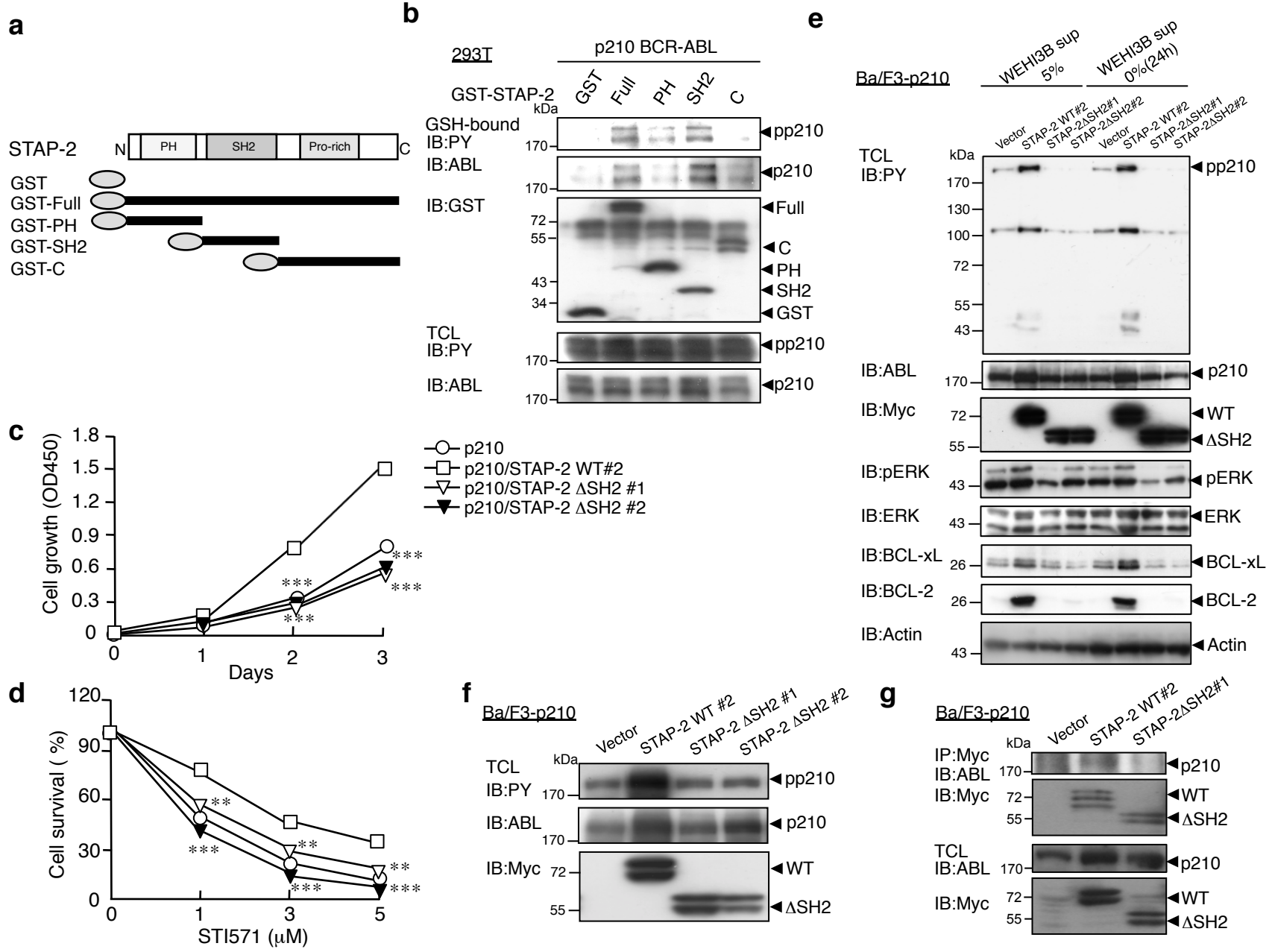
a
STAP-2
N
PH
SH2
Pro-rich
C
GST
GST-Full
GST-PH
GST-SH2
GST-C
b
293T
p210 BCR-ABL
GST-STAP-2
GST
Full
PH
SH2
C
kDa
GSH-bound
IB:PY
IB:ABL
IB:GST
TCL
IB:PY
IB:ABL
pp210
p210
Full
C
PH
SH2
GST
c
Cell growth (OD450)
Days
p210
p210/STAP-2 WT#2
p210/STAP-2 ΔSH2 #1
p210/STAP-2 ΔSH2 #2
d
Cell survival (%)
STI571 (μM)
e
Ba/F3-p210
WEHI3B sup 5%
WEHI3B sup 0%(24h)
Vector
STAP-2 WT#2
STAP-2ΔSH2#1
STAP-2ΔSH2#2
TCL
IB:PY
IB:ABL
IB:Myc
IB:pERK
IB:ERK
IB:BCL-xL
IB:BCL-2
IB:Actin
WT
ΔSH2
pERK
ERK
BCL-xL
BCL-2
Actin
f
Ba/F3-p210
Vector
STAP-2 WT #2
STAP-2 ΔSH2 #1
STAP-2 ΔSH2 #2
g
Ba/F3-p210
IP:Myc
IB:ABL
IB:Myc

Figure 5

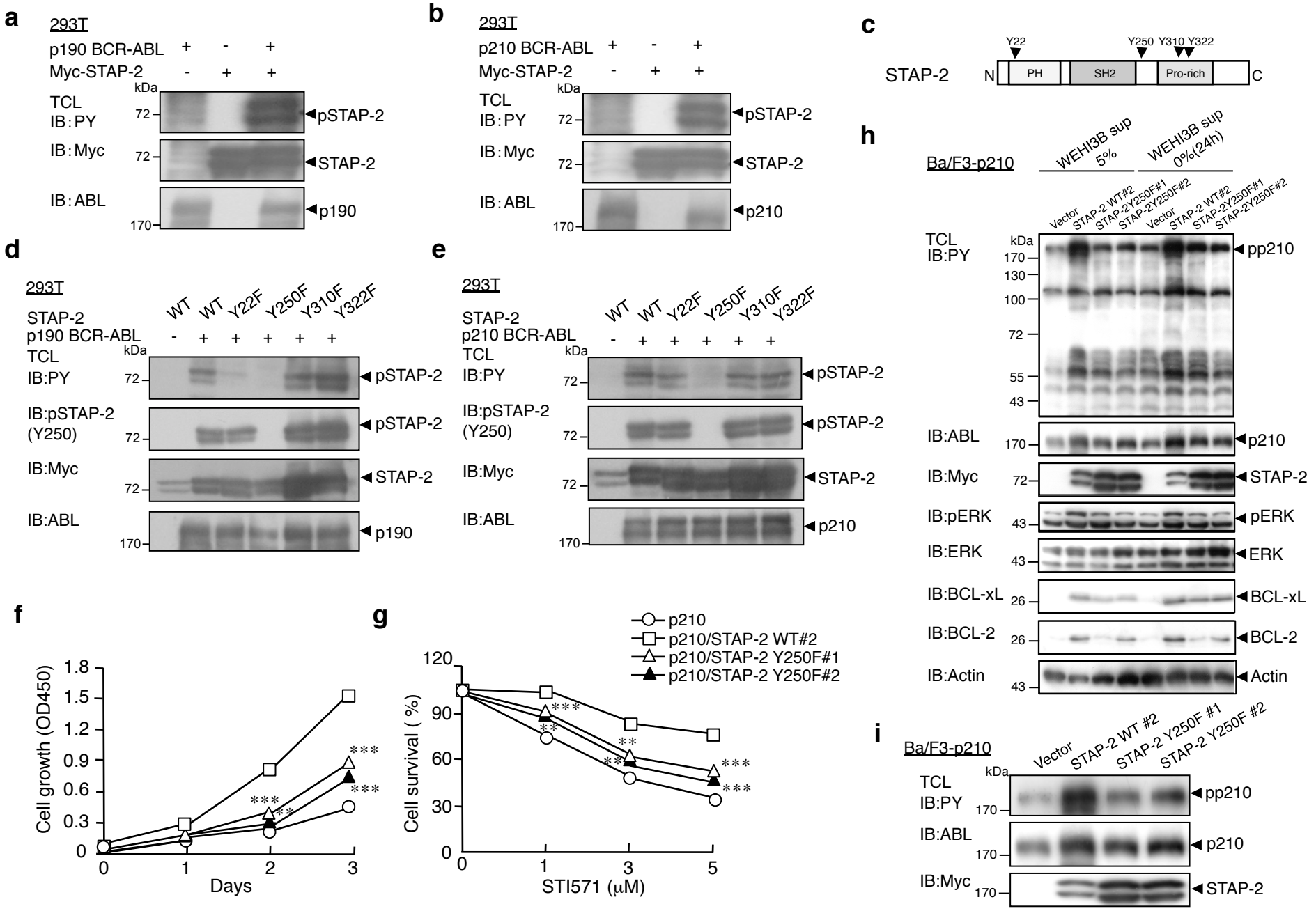
a
293T
p190 BCR-ABL + - +
Myc-STAP-2 - + +
kDa
TCL
IB:PY
72
pSTAP-2
IB:Myc
72
STAP-2
IB:ABL
170
p190
b
293T
p210 BCR-ABL + - +
Myc-STAP-2 - + +
kDa
TCL
IB:PY
72
pSTAP-2
IB:Myc
72
STAP-2
IB:ABL
170
p210
c
Y22
Y250 Y310 Y322
STAP-2
N
PH
SH2
Pro-rich
C
d
293T
WT WT Y22F Y250F Y310F Y322F
STAP-2
p190 BCR-ABL - + + + + +
TCL
kDa
IB:PY
72
pSTAP-2
IB:pSTAP-2 (Y250)
72
pSTAP-2
IB:Myc
72
STAP-2
IB:ABL
170
p190
e
293T
WT WT Y22F Y250F Y310F Y322F
STAP-2
p210 BCR-ABL - + + + + +
TCL
kDa
IB:PY
72
pSTAP-2
IB:pSTAP-2 (Y250)
72
pSTAP-2
IB:Myc
72
STAP-2
IB:ABL
170
p210
f
Cell growth (OD450)
1.8
1.5
1.2
0.9
0.6
0.3
0
0 1 2 3
Days
***
**
g
p210
p210/STAP-2 WT#2
p210/STAP-2 Y250F#1
p210/STAP-2 Y250F#2
Cell survival (%)
120
90
60
30
0
0 1 3 5
STI571 (μM)
h
Ba/F3-p210
WEHI3B sup 5%
WEHI3B sup 0%(24h)
Vector
STAP-2 WT#2
STAP-2Y250F#1
STAP-2Y250F#2
TCL
IB:PY
kDa
170
130
100
72
55
43
pp210
IB:ABL
170
p210
IB:Myc
72
STAP-2
IB:pERK
43
pERK
IB:ERK
43
ERK
IB:BCL-xL
26
BCL-xL
IB:BCL-2
26
BCL-2
IB:Actin
43
Actin
i
Ba/F3-p210
Vector
STAP-2 WT #2
STAP-2 Y250F #1
STAP-2 Y250F #2
TCL
IB:PY
kDa
170
pp210
IB:ABL
170
p210
IB:Myc
170
STAP-2

Figure 6

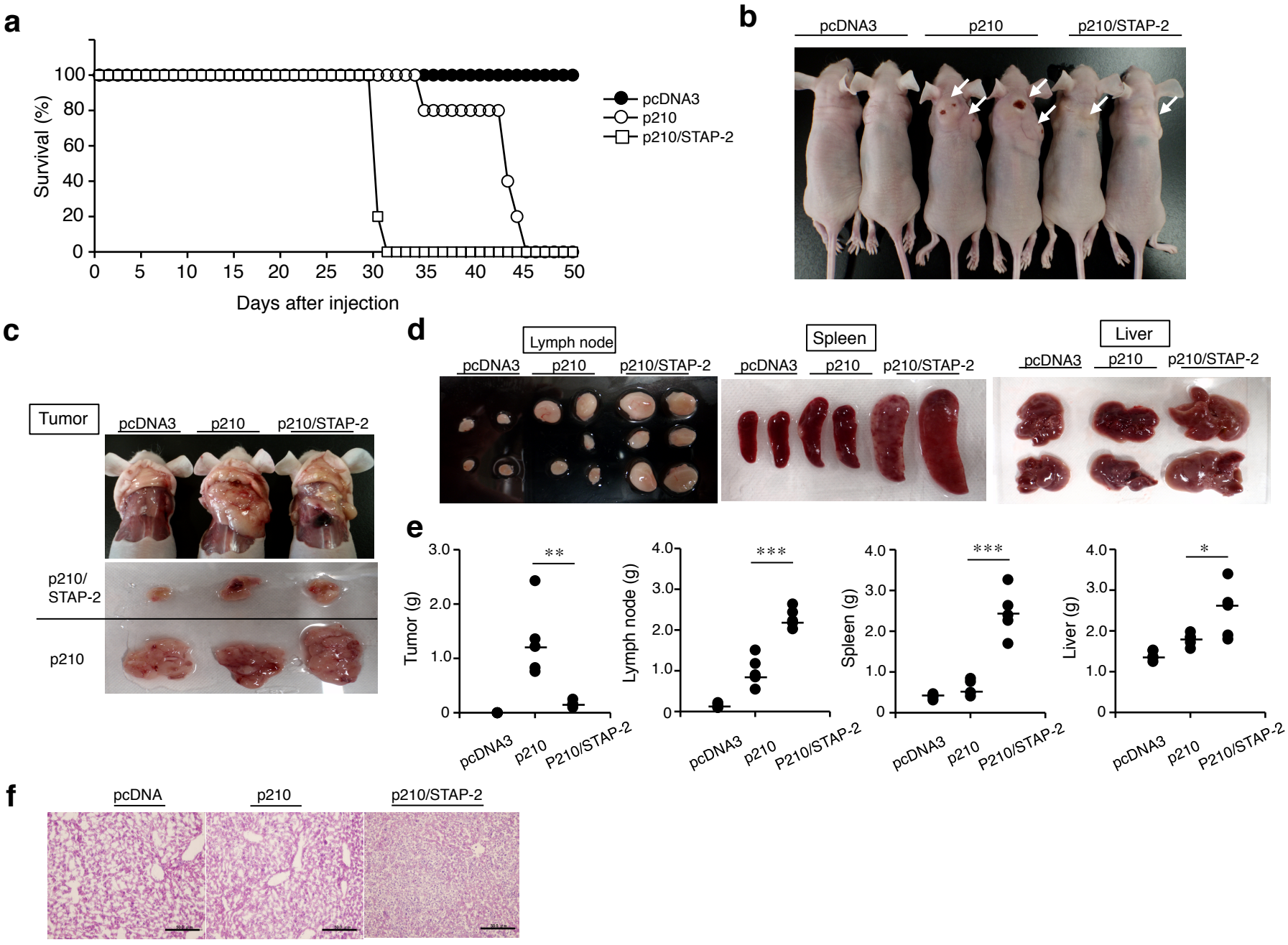
a
Survival (%)
100
80
60
40
20
0
0 5 10 15 20 25 30 35 40 45 50
Days after injection
pcDNA3
p210
p210/STAP-2
b
pcDNA3
p210
p210/STAP-2
c
Tumor
pcDNA3
p210
p210/STAP-2
p210/
STAP-2
p210
d
Lymph node
pcDNA3
p210
p210/STAP-2
Spleen
pcDNA3
p210
p210/STAP-2
Liver
pcDNA3
p210
p210/STAP-2
e
Tumor (g)
3.0
2.0
1.0
0
**
pcDNA3
p210
P210/STAP-2
Lymph node (g)
4.0
3.0
2.0
1.0
0
***
pcDNA3
p210
P210/STAP-2
Spleen (g)
4.0
3.0
2.0
1.0
0
***
pcDNA3
p210
P210/STAP-2
Liver (g)
4.0
3.0
2.0
1.0
0
*
pcDNA3
p210
P210/STAP-2
f
pcDNA
p210
p210/STAP-2

Figure 7

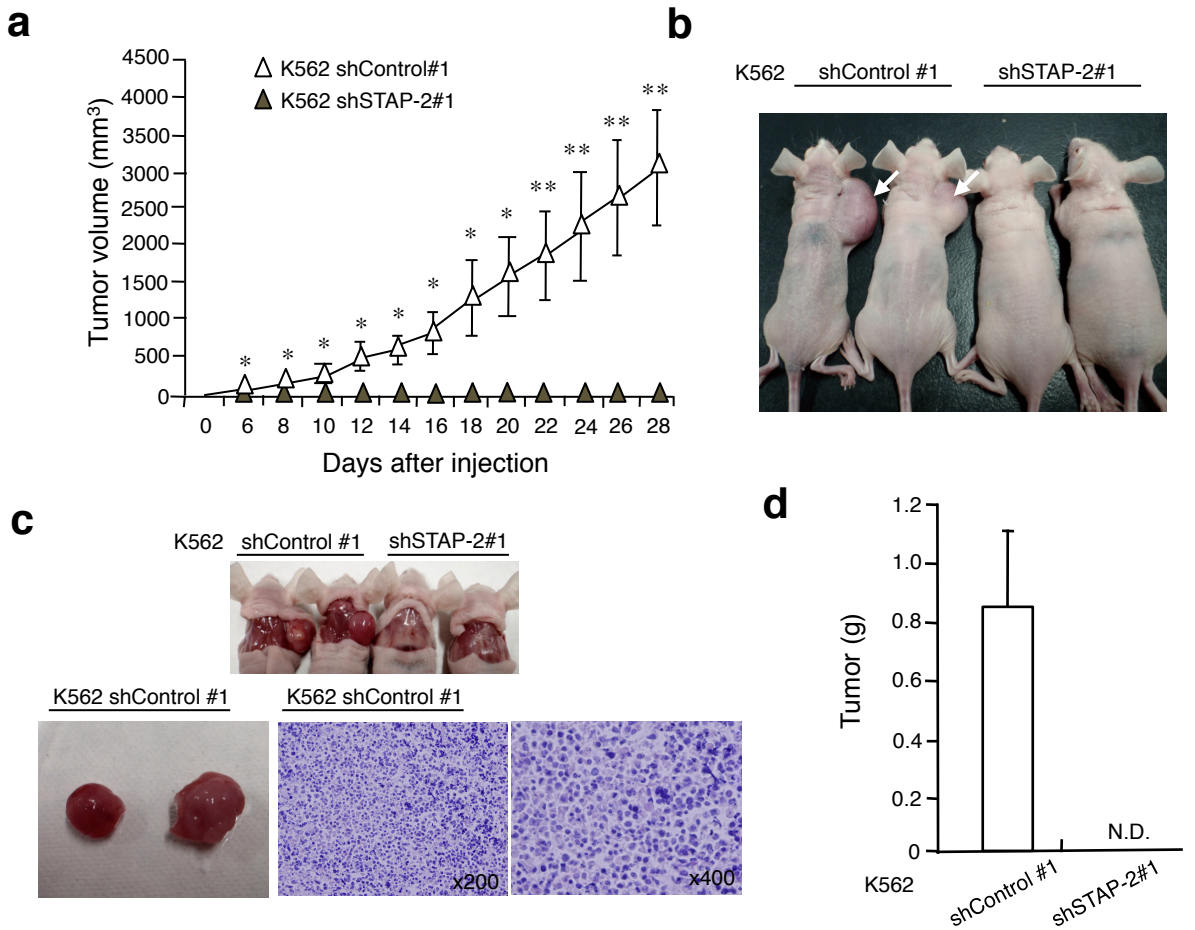
a
b
c
d
K562 shControl#1
K562 shSTAP-2#1
Tumor volume (mm3)
Days after injection
K562
shControl #1
shSTAP-2#1
K562 shControl #1
K562 shControl #1
x200
x400
Tumor (g)
N.D.
K562
shControl #1
shSTAP-2#1

Figure 8

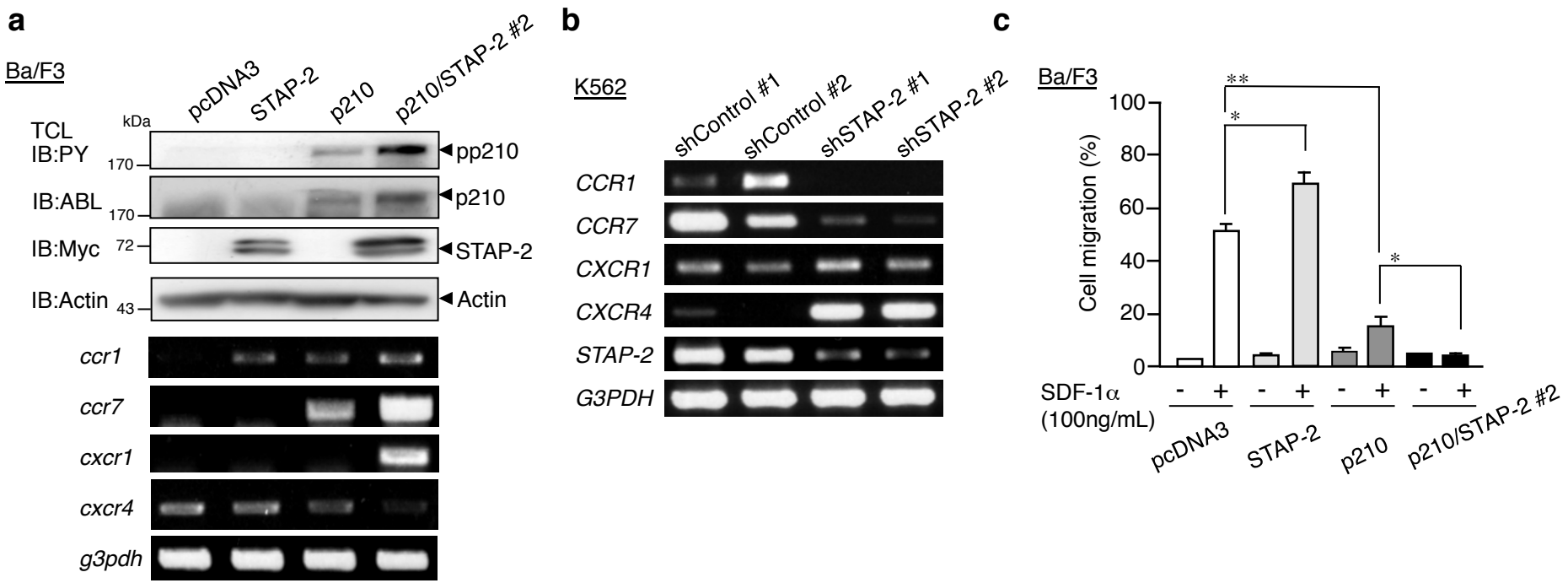
a
Ba/F3
pcDNA3
STAP-2
p210
p210/STAP-2 #2
kDa
TCL
IB:PY
170
pp210
IB:ABL
170
p210
IB:Myc
72
STAP-2
IB:Actin
43
Actin
ccr1
ccr7
cxcr1
cxcr4
g3pdh
b
K562
shControl #1
shControl #2
shSTAP-2 #1
shSTAP-2 #2
CCR1
CCR7
CXCR1
CXCR4
STAP-2
G3PDH
c
Ba/F3
Cell migration (%)
100
80
60
40
20
0
**
*
*
SDF-1α
(100ng/mL)
- + - + - + - +
pcDNA3
STAP-2
p210
p210/STAP-2 #2